REVIEW

Fluorescence nanoscopy at the sub-10 nm scale

Luciano A. Masullo[1,2] · Alan M. Szalai[1] · Lucía F. Lopez[2] · Fernando D. Stefani[1,2]

Abstract

Fluorescence nanoscopy represented a breakthrough for the life sciences as it delivers 20–30 nm resolution using far-field fluorescence microscopes. This resolution limit is not fundamental but imposed by the limited photostability of fluorophores under ambient conditions. This has motivated the development of a second generation of fluorescence nanoscopy methods that aim to deliver sub-10 nm resolution, reaching the typical size of structural proteins and thus providing true molecular resolution. In this review, we present common fundamental aspects of these nanoscopies, discuss the key experimental factors that are necessary to fully exploit their capabilities, and discuss their current and future challenges.

First- and second-generation nanoscopy methods

Super-resolution fluorescence microscopy, also called fluorescence nanoscopy, has overcome the diffraction limit of light and enabled theoretically unlimited spatial resolution in far-field microscopy (Hell et al. 2007; Hell 2015). All nanoscopy methods rely on controlling molecular transitions in the fluorescent probes between bright states (emitting at the detected wavelengths) and dark states (not emitting at the detected wavelengths). Super-resolution is achieved by allowing only a subset of fluorescent markers to be in their bright state at each time point of the measurement. The methods are commonly grouped according to their readout mode. Among the first-generation methods, two families stand out: coordinate-targeted nanoscopies such as Stimulated Emission Depletion (STED) (Klar et al. 2000; Hell

and Wichmann 1994) or Reversible Saturable Optical Fluorescent Transition (RESOLFT) (Hofmann et al. 2005; Hell et al. 2003), and coordinate-stochastic nanoscopies such as Stochastic Optical Reconstruction Microscopy (STORM) (Rust et al. 2006) or Photoactivated Localization Microscopy (PALM) (Betzig et al. 2006). The latter are also known as Single-Molecule Localization Microscopy (SMLM). The principles of these techniques are very well documented (Hell et al. 2007; Huang et al. 2009), and many implementations are nowadays commercially available.

Under ambient or biologically compatible conditions, first-generation techniques achieve a typical resolution of 20–40 nm due to the limited photostability of fluorophores. Such an improved resolution represented a breakthrough for the life sciences because it enabled the visualization of biomolecular assemblies with unprecedented detail and even the discovery of protein supramolecular structures (Sahl et al. 2017). This practical resolution limit has motivated the development of a second generation of fluorescence nanoscopy methods that achieve resolutions in the range of 1 to 10 nm, reaching or surpassing the typical size of structural proteins and providing real molecular resolution.

Conceptually, there are two possible ways to circumvent the photostability limitation: obtaining more fluorescence photons from a given position in the sample or extracting more information from the limited photon budget. Recently, both strategies have been explored by techniques based on coordinate stochastic localization of single molecules. One way to obtain more fluorescence photons from specific

Luciano A. Masullo and Alan M. Szalai contributed equally to this work.

✉ Fernando D. Stefani
fernando.stefani@df.uba.ar

1 Centro de Investigaciones en Bionanociencias (CIBION), Consejo Nacional de Investigaciones Científicas Y Técnicas (CONICET), Godoy Cruz 2390, C1425FQD Ciudad Autónoma de Buenos Aires, Argentina

2 Departamento de Física, Facultad de Ciencias Exactas Y Naturales, Universidad de Buenos Aires, Güiraldes 2620, C1428EHA Ciudad Autónoma de Buenos Aires, Argentina

positions of a sample is through DNA-Points Accumulation for Imaging in Nanoscale Topography (DNA-PAINT). In this SMLM method, programmable transient hybridization of short, fluorescently labeled single-stranded DNA sequences is exploited to repeatedly interrogate positions of the sample with multiple fluorophores, and virtually unlimited fluorescence photons (Schnitzbauer et al. 2017; Jungmann et al. 2010). DNA-PAINT provides a spatial resolution well below 10 nm (Dai et al. 2016; Strauss et al. 2018; Strauss and Jungmann 2020) using standard single-molecule camera-based localization algorithms.

On the other hand, the so-called MINFLUX method (Balzarotti et al. 2017; Masullo et al. 2021) combines concepts of coordinate targeted and coordinate stochastic nanoscopy to attain 1-nm resolution, by enhancing the information carried in each detected photon. After the publication of MINFLUX, a series of techniques using single-molecule localization together with sequential structured illumination (which we will call SML-SSI) have been developed. They all inject the information of the spatial distribution of the excitation light in the localization process. Some of these techniques, namely, modulated localization (ModLoc) (Jouchet, et al. 2021), Repetitive Optical Selective Exposure (ROSE) (Gu et al. 2019), SIMFLUX (Cnossen et al. 2020), and Structured Illumination based Point Localization Estimator with enhanced precision (SIMPLE) (Reymond et al. 2019) have been recently reviewed (Reymond et al. 2020) and a common framework to describe SML-SSI methods has been developed (Masullo et al. 2021). While they should be considered single-molecule localization techniques, they differ from SMLM methods in the illumination used, which is not homogenous but carefully structured and characterized to enhance the localization precision. Moreover, some of the implementations do not use a wide-field detector array (camera) but point-like detectors (e.g. avalanche photodiodes).

The axial resolution in fluorescence nanoscopy is often 2- to 5- fold worse than the lateral counterpart. To date, only a small group of techniques have been able to achieve axial resolutions in the 1–10 nm range. The interferometric detection of single molecules in the, 4Pi configuration makes it possible to reach an axial resolution of around 10–20 nm, but at the expense of high technical complexity (Huang, et al. 2016; Shtengel et al. 2009; Aquino et al. 2011). On the other hand, strategies that localize single molecules based on properties dependent on their distance to a surface are likely to achieve high axial resolution in the vicinity of the interface. Supercritical Illumination Microscopy Photometric z-Localization with Enhanced Resolution (SIMPLER) (Szalai et al. 2021) is a technique capable of reaching sub-10 nm axial resolution with a conventional total internal reflection (TIR) microscope, by calibrating the z-dependent signal from single emitters considering the excitation through the TIR evanescent field and the modulation of the emission angular pattern by the interface (Szalai et al. 2021). In Supercritical Angle Localization Microscopy (SALM), the super-critical angular emission is the key property that encodes the axial position (Bourg et al. 2015). Performed with high numerical aperture objectives ($NA = 1.70$) and high-refractive index coverslips and immersion oil, SALM can reach sub-10 nm axial precision (Dasgupta et al. 2021). Methods that exploit the distance-dependent energy transfer to a conductive surface, determine the axial position of fluorophores from lifetime measurements (Chizhik et al. 2014). Particularly, methods using graphene-covered substrates (graphene energy transfer, GET) reach sub-10 nm localization precision (Ghosh et al. 2019; Kaminska et al. 2019; Kamińska et al. 2021). Finally, the SML-SSI methods described before can also be applied to localize molecules in the axial direction with sub-10 nm resolution, as demonstrated by 3D-MINFLUX (Gwosch et al. 2020), ModLoc (Jouchet et al. 2021), and ROSE-Z (Gu et al. 2021).

Quantifying spatial resolution

In addition to the particular features of each method, the spatial resolution achieved in real-life experiments is influenced by multiple experimental factors, such as sample drift, size and structure of the labels, or readout noise of the detectors. Therefore, it is necessary to determine the resolution experimentally.

Until today, there is no standard procedure to quantify the resolution of fluorescence nanoscopy images. First works usually reported the achieved resolution in terms of the full width at half maximum of the smallest structures or features of the image (Huang et al. 2008; Willig et al. 2007; Rittweger et al. 2009; Heilemann et al. 2008). While such values provide valid performance examples, it should be noted that the resolution of a super-resolved image may vary from point to point of a sample. For example, in STED, the achievable resolution depends on the efficiency of depletion, which in turn depends on the local intensity and polarization of the depletion laser, and on the orientation and emission spectrum of the molecules involved. In SMLM, the localization precision varies from molecule to molecule because each one delivers a different number of fluorescence photons. Thus, in general, the resolution of a fluorescence nanoscopy image is not a single value but a distribution, which should be characterized. To date, different algorithms have been proposed to quantify the average resolution from a complete image (Nieuwenhuizen et al. 2013; Descloux et al. 2019; Descloux et al. 2021). We note that, in methods that include an image renderization step, such as SMLM, the determined average resolution may be influenced by the particular renderization algorithm. Also, in this regard, there is no established standard to render super-resolution images from single-molecule localization data.

An alternative approach to demonstrate resolution and to obtain a resolution distribution consists of measuring calibration standards containing fluorescent markers at well-known positions. DNA origami are greatly suitable to fabricate this kind of standards as they enable the organization of individual fluorophores at predefined distances with nanometer precision, both statically and dynamically (Schmied et al. 2014; Scheckenbach et al. 2020). DNA origami standards have been widely used to characterize the super-resolution performance of various methods. Figure 1 includes examples of MINFLUX (Fig. 1a) (Balzarotti et al. 2017), p-MINFLUX (Fig. 1b) (Masullo et al. 2021), DNA-PAINT (Fig. 1c) (Strauss and Jungmann 2020), and ROSE (Fig. 1d) (Gu et al. 2019). Moreover, three-dimensional origamis have also been developed to benchmark the 3D sub-10 nm techniques, such as the combination of graphene energy transfer and DNA-PAINT, as shown in Fig. 1e, where features separated 2.7 nm in the axial direction were resolved (Kamińska et al. 2021). DNA origami offer enormous versatility in terms of geometries and functionalities that can be used. As disadvantage, the calibration with DNA origami may be slightly inaccurate because DNA structures present some degree of flexibility. Also, the linkage of the fluorophores used in the calibration samples may differ from the one used in the target biological sample.

Alternatively, highly stable natural supramolecular protein structures with well-defined nanometric geometries are abundant in biological cells, and may serve as in-situ calibration standards (Fig. 1f–l). For example, the nuclear pore complex (NPC) is a suitable structure to determine the resolution of fluorescence nanoscopy methods both in 2D and 3D (Schlichthaerle et al. 2019; Thevathasan et al. 2019). The NPC is a protein assembly consisting of three rings: an inner ring complex, a cytoplasmic ring, and a third ring located in the nuclear side. It contains copies of approximately 30 different nucleoporins (Appen et al. 2015). A usual strategy consists of imaging the distribution of the nucleoporins Nup96 or Nup107 (Loïodice et al. 2004), present in the nuclear and cytoplasmic rings of the NPC of vertebrates, which are organized in clusters forming a regular octahedron with a side of ~42 nm. Each cluster is composed of two nucleoporins separated by around 12 nm (see schematic in Fig. 1f). The nuclear and cytoplasmic rings are parallel to the nuclear membrane and separated by a distance of ~50 nm for Nup96 (Thevathasan et al. 2019) and ~60 nm for Nup107 (Heydarian et al. 2021). In the area of the nuclear membrane parallel to the sample substrate, the structure of the NPC represents a unique platform to benchmark the performance of nanoscopy methods in 2D and 3D, with well-defined distances ranging from 10 to 60 nm, approximately. Figure 1g shows images of the Nup96 acquired using 3D DNA-PAINT (Schlichthaerle et al. 2019), while Fig. 1h presents images of the same structure obtained

with MINFLUX (Gwosch et al. 2020). In 3D-MINFLUX, Nup96 was localized axially with ~2 nm precision, and the 50 nm-separation was accurately retrieved (Schmidt et al. 2021) (Fig. 1i). Aiming at broadening the access to this reference standard, genome edited cell lines were recently developed, in which nucleoporin Nup96 was endogenously labeled with different tags (Thevathasan et al. 2019). Other well-defined supramolecular protein structures can also be used to test the performance of nanoscopy methods. Microtubules, for instance, are a cylindrical and hollow structure formed by the assembly of α-/β-tubulin heterodimers, with an external diameter of ~25 nm (Fig. 1j) that can scale up to 40–50 nm when labeled (the actual diameter depending on the labeling strategy). Microtubule cross-sections were used as calibration standards to demonstrate the performance of several methods (Jouchet, et al. 2021; Szalai et al. 2021; Gu et al. 2021; Li et al. 2018; Huang et al. 2016). An example is shown in Fig. 1k, where images of fully resolved hollow cross-section of single microtubules were used to demonstrate that SIMPLER combined with DNA-PAINT can reach sub-10 nm resolution in the three dimensions of biological samples (Szalai et al. 2021). 4Pi-SMLM has been shown to provide almost isotropic resolution of 10–20 nm by resolving the hollow structure of microtubules (Fig. 1l) (Huang, et al. 2016).

Sample drift

All microscopes suffer from thermo-mechanical instabilities that produce undesired misalignments of the setup. For microscopy, the most critical one is the displacement of the sample with respect to the objective of the microscope, which is commonly called sample drift. A well-built microscope presents sample drifts in the order of a few nm per minute, typically. While this level of drift is insignificant for most diffraction-limited imaging situations and for fast super-resolution methods like STED, it becomes a serious bottleneck for slower methods like SMLM and SML-SSI aiming to achieve sub-10 nm resolution.

There are basically two ways to correct for sample drift: post-processing corrections and active corrections during the measurement. A basic post-processing drift correction that is often applied in SMLM consists of determining the sample motion by correlation between subsequent images (Wang et al. 2014). This correction can only compensate long timescale drift because several frames must be used to obtain a partial image of sufficient quality to perform a sensible correlation. A more accurate correction is obtained by introducing fiducial markers into the sample (micro or nanoparticles detectable by scattering, photoluminescence, fluorescence, or transmission) (Rust et al. 2006; Betzig et al. 2006; Balinovic et al. 2019). The positions of the fiducial markers are registered in time through the same super-resolution
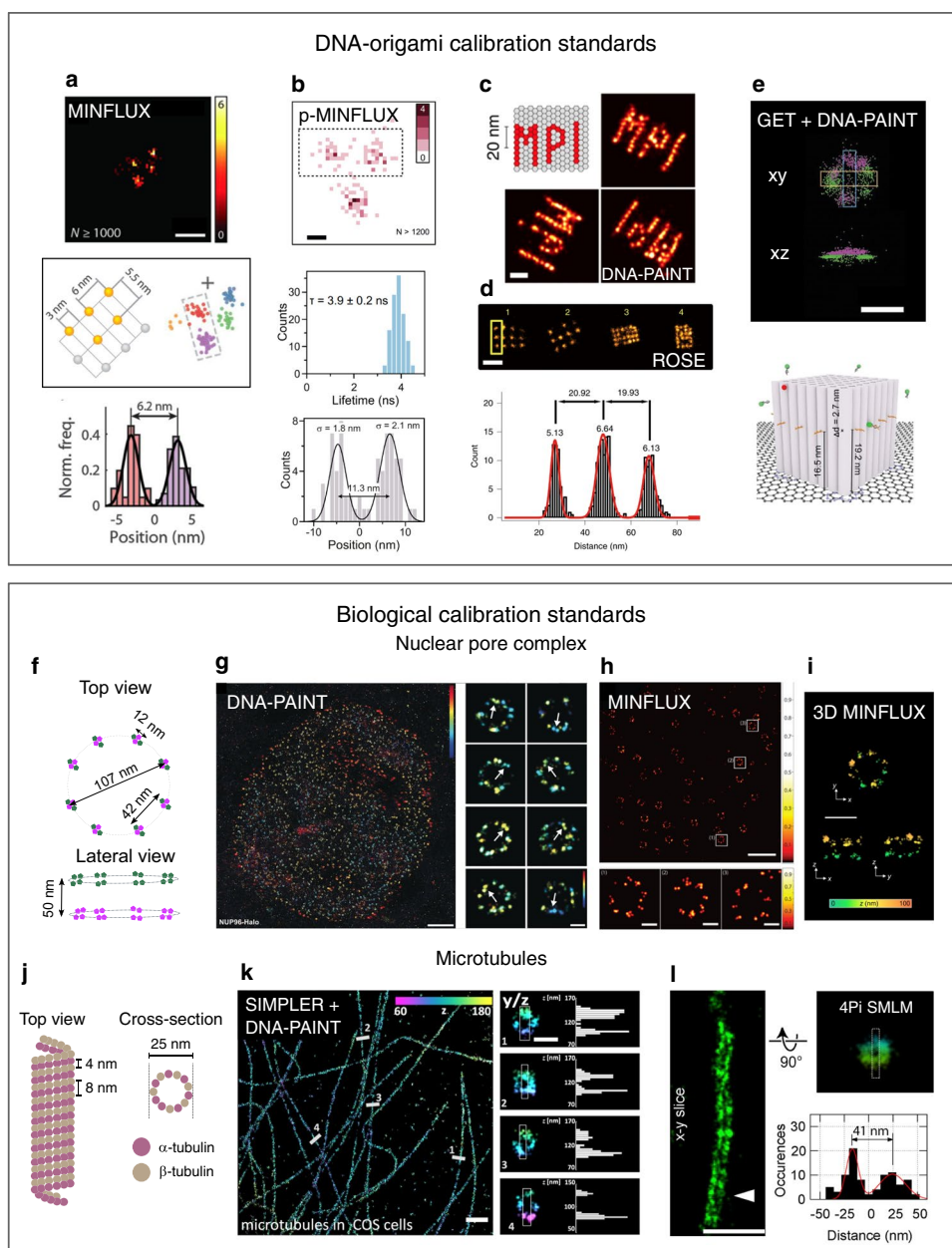
Fig. 1 Examples of the performance of some sub-10 nm resolution nanoscopy methods using DNA origami (**a–e**) and biological calibration standards (f-l). **a** MINFLUX images of DNA origami structures showing ~1–2 nm resolution (adapted from (Balzarotti et al. 2017)). **b** p-MINFLUX localizations and lifetime data of a DNA origami structure (adapted from (Masullo et al. 2021)). **c** DNA-PAINT images of a DNA origami structure used to demonstrate 5-nm resolution (adapted from (Strauss and Jungmann 2020)). **d** Images of DNA- origami structures obtained using ROSE, demonstrating 5 nm resolution (adapted from (Gu et al. 2019)). **e** GET + DNA-PAINT images of a cubic DNA origami structure, where ~3 nm axial resolution is proved (adapted from (Kamińska et al. 2021)). **f** Schematic of the NPC molecular structure. **g** 3D DNA-PAINT images of the Nup96-HALO in a whole cell nucleus and selection of single NPCs (adapted from (Schlichthaerle et al. 2019)). 12 nm distances between neighboring Nup96 are resolved. **h** MINFLUX images of NPCs in a U-2 OS cell (adapted from (Gwosch et al. 2020)). **i** 3D MINFLUX images of an individual NPCs in U-2 OS cells (adapted from (Schmidt et al. 2021)). **j** Schematic of the microtubule molecular structure. **k** SIM-PLER + DNA-PAINT images of microtubules in COS7 cells, where sub-10 nm-axial resolution allows fully resolving the cross-sections of single microtubules (adapted from (Szalai et al. 2021)). **l** 4Pi-SMLM image of a microtubule at ~10 nm resolution shows the hollow structure clearly resolved (adapted from (Huang, et al. 2016)). Scale bars: **a** 10 nm, **b** 5 nm, **c** 20 nm, **d** 50 nm, **e** 30 nm, **g** 2 μm (left) and 50 nm (right), **h** 500 nm (top) and 50 nm (bottom), **k** 1 μm (left) and 50 nm (right), **l** 300 nm

measurement or independently, and are subsequently used to correct the sample position in a post-acquisition analysis (Fig. 2a). The more fiducial markers used, the more accurate the correction will be. Advanced post-processing drift correction methods using DNA origami as fiducial markers and particle averaging algorithms have made it possible to achieve sub-5 nm resolution in DNA-PAINT (Dai et al. 2016) but this method requires having several hundreds of DNA origami per field of view in addition to the biological structure. Post-processing drift corrections are limited to in-plane lateral drifts (x, y) and should be complemented with an active correction for the axial position (z). Using the lateral displacement of an auxiliary infrared focused beam that is incident on the sample in total internal reflection is a typical strategy to lock the sample in focus. In this way, axial stabilization with precision down to 5 nm can be achieved. It is worth to mention that those 3D nanoscopy methods that estimate the axial position of single molecules from a signal that depends on the distance to an interface, such as SIMPLER, SALM, or GET, are unaffected by the axial drift. In contrast, the capability of 3D-MINFLUX, ModLoc, or ROSE-Z to achieve sub-10 nm axial resolution depends critically on the stability of the microscope, and usually require active (x, y, z) drift correction.

Sample drift can be actively corrected in real-time with a feedback loop by tracking the position of fiducial markers in the sample and correcting the sample-objective relative position with a piezoelectric stage (Fig. 2a). In this way, stabilization precisions of ~ 1nm or better can be achieved in the three dimensions (Carter 2007; Pertsinidis et al. 2010), limited mainly by the localization precision of the fiducials and the resolution of the piezoelectric stage. For the axial correction, a z-dependent imaging scheme should be implemented such as astigmatic imaging. Simple, cost-efficient, high-performance (x, y, z) stabilization systems have been proposed recently (Balzarotti et al. 2017; Masullo et al. 2021; Schmidt et al. 2021; Coelho et al. 2020) and some of them are open-source hardware implementations (Masullo et al. 2021; Coelho et al. 2020) that have the potential to be implemented in many existing optical systems. We note that actively stabilizing the system is fully compatible with carrying out a further post-acquisition drift correction which allows to correct residual drift that might have not been actively corrected.

Labeling strategy

Exploiting the full potential of advanced nanoscopy methods calls for decorating biological targets with nanometer precision and high density, a biochemical challenge not yet achieved in most super-resolution experiments. The most used labeling strategy is indirect immunostaining. Immunoglobulin G (IgG) antibodies have molecular weights of 150 kDa and a size of approximately ~ 7 nm, resulting in a total distance between the targeted protein and the fluorophore of 10–15 nm or more (Ganji et al. 2021; Früh et al. 2021). As the orientation and stoichiometry of the primary/secondary antibody conjugation is impossible to control, this strategy leads to an increase in the localization uncertainty, as shown schematically in Fig. 2b, impairing the possibility of achieving sub-10 nm resolution. Moreover, the steric hindrance produced by the combination of primary/secondary antibodies also limits the achievable labeling density.

One way to decrease the linkage error is to directly label primary antibodies with fluorophores or DNA handles for DNA-PAINT. The main disadvantage of this approach is the need to conjugate fluorophores or oligonucleotides to specific antibodies for each target. Alternatively, antigen-binding fragments (Fab) can be used to decrease the size of the labels from 150 to 50 kDa. Combining primary full IgG antibodies with secondary Fab fragments outcomes a linkage error comparable to the one achieved when using directly labeled primary antibodies. Recently, a pipeline for site-specific labeling of antibodies has been shown to increase the control over the stoichiometry and localization of the markers, which is useful for understanding and minimizing linkage error (Früh et al. 2021).

In recent years, small-sized affinity reagents including nanobodies (Schlichthaerle et al. 2019; Ries et al. 2012; Pleiner et al. 2015), affimers (Schlichthaerle et al. 2018), aptamers (Strauss et al. 2018), small binding molecules (Wang et al. 2019), and genetically encoded self-labeling enzymes (e.g. SNAP-Tag, Halo-Tag) (Keppler et al. 2003; Los et al. 2008) have improved the final resolution achieved in fluorescence nanoscopy. However, all these strategies have limitations that still need to be addressed before they are routinely applied.

Nanobodies are single-domain antibodies with typical molecular weights of 12–15 kDa and sizes of 2–3 nm but their availability is limited to a small population of targets, and developing new ones is costly and requires complex steps not available in most laboratories, such as immunization of animals. A typical procedure to address the restricted availability of nanobodies consists of fusing the target protein with GFP and using well established anti-GFP nanobodies, which has the drawback of increasing the label size by ~ 40 kDa. On the other hand, self-labeling enzymes allow covalent labeling of fusion proteins with small and bright organic dyes. A disadvantage of these strategies is that they involve the genetic modification of cell lines (through, for example, CRISPR Cas technology), in which the expression level of the targeted protein has to be carefully characterized in order to avoid potential artifacts.

Affimers are 2 nm-sized proteins (10–12 kDa) that can act as binding agents similarly to antibodies (Tiede et al. 2017). Tubulin (Tiede et al. 2017) and actin (Schlichthaerle et al. 2018) affimers have been successfully developed and tested

Fig. 2 Key experimental factors for sub-10 nm resolution nanoscopy. **a** Drift correction can be performed either actively or by post-acquisition processing. The former strategy keeps the sample in a fixed position with nanometer or sub-nanometer precision, while the latter lets the sample drift freely (often hundreds of nanometers) and corrects the position of each detected molecule during the data analysis, considering the trajectory of the fiducial markers. **b** Labeling strategies are critical in the final achieved resolution. Bulky labels, such as the combination of primary and secondary antibodies, prevent reaching sub-10 nm resolution. In contrast, small labels (e.g. nanobodies, affimers, aptamers, self-labeling enzymes) introduce minimal linkage errors (3–4 nm). **c** Detecting with low noise, low darkcounts, single-photon detectors such as avalanche photodiodes (blue) produces data with only Poisson noise. Devices such as EMCCD or sCMOS cameras add significant readout noise to the measurement (orange), increasing the uncertainty in the position estimation
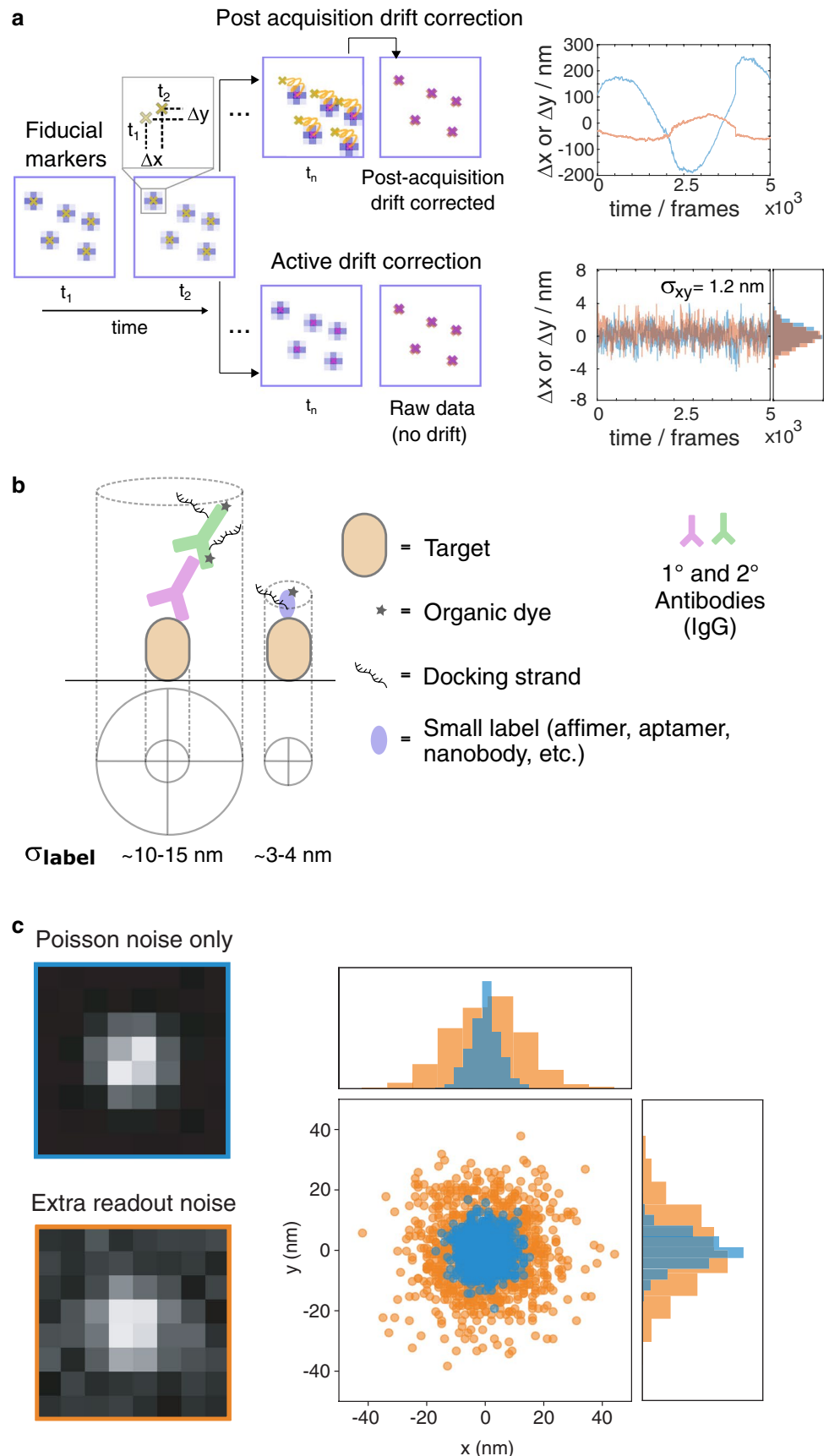
in dSTORM and DNA-PAINT, reaching minimal linkage errors. Similarly, aptamers are single-stranded DNA or RNA molecules that can bind specifically to targets (Opazo et al. 2012) and have been recently used as labeling reagents in DNA-PAINT measurements, allowing to achieve sub-10 nm resolution in biological samples (Strauss et al. 2018). While both strategies have great potential to be utilized in super-resolution microscopy methods, their use is still in an early stage and only few targets have been labeled with them so far (Strauss et al. 2018; Schlichthaerle et al. 2019; Bedford et al. 2017). In both cases, high-throughput screening is needed to find suitable affinity reagents candidates.

Finally, small fluorophores can also be used to directly bind to the targets through specific interactions. Although this is a laborious route for each specific target, there are successful examples. Fluorogenic cell-permeable probes have been developed to label the cytoskeleton proteins actin and tubulin in live cells (Lukinavičius et al. 2014). These silicon-rhodamine (SiR) derivatives (Lukinavičius et al. 2013) (SiR-actin and SiR tubulin) allow, for example, to perform live-cell STED imaging (D'Este et al. 2015). On the other hand, phalloidin is a widely used reagent capable of binding filamentous actin (F-actin) (Dancker et al. 1975), the use of which has allowed imaging actin filaments with ~ 13 nm resolution (Schlichthaerle et al. 2018). Moreover, small fluorescent markers of membrane receptors have been developed, either by labeling small receptor agonist or antagonist with organic dyes (Hern and a, 2010; Cai et al. 2004), or by designing a specific fluorophore capable of acting as an antagonist itself, i.e. being able to directly bind to the receptor (Szalai et al. 2018).

Signal, background, and detector noise

For all methods, the localization precision of single molecules scales with the number N of photons used for the localization as $\sim 1/\sqrt{N}$, and improves with increasing SBR and SNR (signal to background ratio and signal to noise ratio). The photophysics of fluorescent probes and their use in super-resolution microscopy is a very well documented topic (Ha and Tinnefeld 2012; Vogelsang et al. 2010; Dempsey et al. 2011; Linde et al. 2012), so we will just mention a few important aspects. As a rule of thumb, organic dyes are brighter and more photostable ($N \sim 10^3 - 10^4$) than fluorescent proteins ($N \sim 10^2 - 10^3$), which is why they are preferred for sub-10 nm nanoscopy. Additionally, it is remarkable how certain imaging buffers can modulate the performance of fluorophores. It is well established that reducing and oxidizing agents in dynamic equilibrium can suppress photoblinking, thus allowing to collect more fluorescence photons per single molecule (Ha and Tinnefeld 2012; Vogelsang et al. 2008). The most spread reagent used for this purpose is Trolox. When this compound is dissolved

in the imaging solution, it is partially converted into Trolox-quinone, which plays the role of reductant, while the remaining unconverted Trolox is the oxidant (Cordes et al. 2009). Furthermore, the removal of oxygen from the solution is crucial to increase the photostability of the fluorescent probes. To this end, enzymatic oxygen scavenging systems are widely used, such as the combination of glucose oxidase, glucose, and catalase (Harada et al. 1990). Alternatively, protocatechuic acid and protocatechuate-3,4-dioxygenase can also be used to reduce the oxygen concentration, with the comparative advantage of avoiding a drop in the pH of the solution over time (Aitken et al. 2008).

Oxidizing and reducing systems, including both Trolox and an oxygen scavenger, are suitable for STED nanoscopy, where they enable several STED acquisitions down to the single molecule level (Szalai et al. 2021; Kasper et al. 2010). Moreover, it is an excellent strategy to be applied in DNA-PAINT measurements, where it helps to increase the number of emitted photons before the unbinding of imager strands. In addition, it prevents the photo-induced damage of binding sites (Blumhardt, et al. 2018). However, this reagent is not suited for STORM because it blocks the required transition to long-lived redox dark states of most fluorophores. An attractive alternative for STORM measurements is the use of polyunsaturated hydrocarbon cyclooctatetraene (COT), which can increase photon yields of the dye AlexaFluor-647 (the best performing dye for STORM (Dempsey et al. 2011)), without compromising its blinking behavior (Olivier et al. 2013).

Despite being a technique in which large number of fluorescence photons can be collected, DNA-PAINT suffers from high background levels due to the presence of freely diffusing imager strands in the imaging buffers. While decreasing the concentration of imager strands reduces the background, this also reduces the frequency of binding events and leads to longer acquisitions times. Recent efforts to diminish background and increase imaging speed in DNA-PAINT have allowed reaching sub-10 nm resolution (Hofmann et al. 2005). These strategies include modifying the salt concentration of the imaging buffers (Schueder et al. 2019), introducing repetitive motifs in the capturing strands (Strauss and Jungmann 2020; Civitci et al. 2020), using fluorogenic probes (Chung, et al. 2020), or implementing Förster resonance energy transfer (FRET) approaches that allow increasing imager strands concentrations without affecting the background level (Lee et al. 2017; Auer et al. 2017).

Many second-generation methods rely on an estimation of the expected detected photons (λ_i) in a given time interval. In camera-based approaches, λ_i corresponds to the expected detected photons in each pixel. In SML-SSI, λ_i corresponds to the i different exposures used in the sequential structured excitation. Intrinsically, photon counting is Poisson

distributed. Thus, the detected photon counts for each exposure or pixel with an ideal detector is $n_i \sim \text{Poisson}(\lambda_i)$. For single-photon counting detectors such as avalanche photodiodes (APD), the pure Poisson noise is a good approximation. However, this is not true for CCD, EM-CCD, or sCMOS cameras in which the number of detected photons presents higher variability and follows a more complex statistical distribution due to the convolution of additional readout and/or amplification noise with Poisson noise (Mortensen et al. 2010; Huang et al. 2013). Thus, experimental schemes that detect the fluorescence photons using APDs or future advances in camera technologies and position sensitive single-photon detectors have the potential to boost the localization precision and hence the spatial resolution of super-resolution methods (Fig. 2c).

Temporal resolution, live cell imaging, and single molecule tracking

Among the first generation super-resolution methods, coordinate-targeted are naturally faster and were first to demonstrate video-rate live imaging of biological specimens (Westphal et al. 2008). Parallelized STED (Bergermann et al. 2015) and RESOLFT (Masullo, et al. 2018; Bodén et al. 2021) implementations have greatly helped increasing the throughput and frame-rate of super-resolution imaging. SMLM methods, on the other hand, are intrinsically slower as their time resolution is limited by the switching kinetics of fluorophores, constraining their applicability to either fixed samples, or a restricted number of live cell imaging applications. Nonetheless, making proper use of fast sCMOS cameras, video-rate SMLM has been demonstrated (Huang et al. 2013).

All methods of the second generation reaching sub-10 nm resolution involve stochastic single-molecule localization and thus share with SMLM the time resolution limitations. As mentioned above, recent advances that reduce the background of the imager solution have speeded-up DNA-PAINT, roughly matching the imaging velocity achieved in STORM (Strauss and Jungmann 2020; Schueder et al. 2019; Civitci et al. 2020; Chung, et al. 2020; Lee et al. 2017; Auer et al. 2017). While the final performance is still too slow to capture the dynamics of most biological processes, there seems to be room for improvement, still. Interestingly, deep and machine learning-based methods have been shown to help reducing the time required to obtain super-resolved images (Ouyang et al. 2018). Another novel approach uses a protein that pre-orders the imager strands in solution and enables a tenfold faster binding (Filius et al. 2020). Among the new generation methods reviewed here, MINFLUX is the only one that has been performed in live cells, by imaging the Nup96–mMaple construct (Gwosch et al. 2020). It should be noticed, however, that the nuclear pore complex had to remain still in the timescale of minutes, and that more

dynamic structures will still be elusive if no substantial improvement in the switching kinetics is achieved.

Single-molecule tracking, while not a super-resolution imaging technique per se, is a relevant tool to investigate biological phenomena in live-cell systems (Enderlein 2000; Weigel et al. 2011; Sako et al. 2000). In this regard, MINFLUX holds a unique potential due to its high photon efficiency, which together with the fast response of APDs allow tracking single molecules with both high temporal and spatial resolution. For example, 30S ribosomal subunit proteins fused to mEos2 was tracked in living *Escherichia coli* at 8 kHz (Balzarotti et al. 2017) with a localization precision of ~50 nm (using just 9 photons per localization). In turn, this enabled the computation of diffusion coefficients at video-rate, providing unprecedented insight into the diffusion behavior of proteins. MINFLUX has also been demonstrated to attain localization precisions of 2nm at $400 \mu s$ time resolution (Eilers et al. 2018). Interestingly, p-MINFLUX is unique among single-molecule localization methods since it can reach the absolute time resolution limit posed by the emission rate of the emitter because the sequential structured excitation is performed at the repetition rate of the pulsed laser (Masullo et al. 2021). Also, p-MINFLUX delivers the fluorescence lifetime, which can be used to obtain information about molecular interactions and local environment. Apart from applications in ultrafast tracking of fluorescent molecules, we believe that p-MINFLUX can become a method of choice to track small (~10nm) metallic or fluorescent nanoparticles or quantum dots. Metallic NPs are particularly interesting since their photoluminescence presents very high emission rates and very short lifetimes, thus allowing to increase the speed of the tracking measurement up to the limit posed by the single-photon detectors.

Finally, we note that single-molecule FRET and diffraction-limited FRET imaging have been widely used to investigate dynamic processes involving changes in distances in the 1–10 nm range (Piston and Kremers 2007; Lerner 2018). Recently, super-resolved FRET imaging was successfully demonstrated based on DNA-PAINT (Deußner-Helfmann et al. 2018) and STED measurements (Tardif et al. 2019; Szalai et al. 2021). In particular, the intensity-based STED-FRET approach (Szalai et al. 2021) enables the observation of FRET dynamics in super-resolved observation volumes, providing an interesting combination of visualization/localization of FRET events with ~40 nm resolution, with FRET dynamics delivering sub-10 nm information with ms temporal resolution.

Conclusions and future perspectives

The development of fluorescence nanoscopy methods and protocols has evolved impressively during the past decade,

particularly in pushing the achieved resolution into the sub-10 nm regime. New approaches, combining the use of sequential structured illumination with the detection of single molecules, have enhanced the spatial resolution by increasing the information carried by each photon, ultimately reaching the molecular scale. Many features and limitations of these techniques are also present in older nanoscopies. Thus, different strategies that have been followed to improve first-generation nanoscopy methods will surely be useful to improve the performance of new generation nanoscopies. For example, developing brighter, smaller, and more stable fluorescent labels with suitable switching kinetics and compatible with live-cell imaging (Wang et al. 2019; Linde et al. 2012; Fernández-Suárez and Ting 2008; Grimm et al. 2020), or finding general strategies to decrease background levels are improvements from which the entire super-resolution field can benefit. Furthermore, analysis based on machine and deep learning represents an appealing route to increase the throughput of nanoscopies. The combination of fluorescence nanoscopy with the so-called expansion microscopy (Chen et al. 2015) is also a straightforward way to maximize the resolution of every nanoscopy method. Nonetheless, to achieve sub-10 nm resolution, the key experimental factors reviewed in this article, namely, mechanical stabilization, labeling strategies, and detector noise are critical.

The throughput of the techniques has also raised permanent interest of the nanoscopy community. Important steps were taken in this direction, allowing SMLM-based nanoscopy to be performed in areas of $\sim 200 \times 200 \mu m^2$ under homogeneous illumination (Mau et al. 2021; Stehr et al. 2019). While the imaging field of view in the first MIN-FLUX implementation was limited to ~ 50–100 nm, a later iterative approach enabled scaling it up to a few micrometers (Gwosch et al. 2020). Thus, MINFLUX still has a way to go regarding the throughput compared to camera-based techniques. In contrast, MINFLUX has proved to be the best choice for ultraprecise single molecule tracking. With respect to the third dimension, techniques depending on the distance to the interface such as SIMPLER, SALM, or GET, while having excellent performances close to the interface, they are limited in depth, and other alternatives (e.g. Mod-Loc or ROSE-Z) should be used to study molecules located at micrometers far from the coverslip.

Sub-10 nm nanoscopy has enormous potential to enable biological studies with molecular resolution and provide key information relevant to big open questions in life sciences. For example, neighboring EGFR proteins labeled with aptamers and separated one from each other 14–16 nm were resolved thanks to the capabilities of DNA-PAINT and the small size of the labels (Strauss et al. 2018). Dual-color 3-D MINFLUX allowed to study the mitochondrial contact site and cristae organizing system with ultra-high precision, shedding light into the nanometer-scale arrangement of Mic60 and Mic19 proteins (Pape et al. 2020). However, its widespread application in biology labs remains challenging. While technical improvements will keep coming and increasing the quality and performance of these techniques, bridging the gap between the nanoscopy and cell biology communities should also be a priority.

Studying living cells at sub-10 or even sub-20 nm resolution remains challenging for most fluorescence nanoscopy methods. While MINFLUX has taken first steps in this direction, both in imaging and tracking applications, the full potential of live-cell nanoscopy at 1–10 nm spatial and sub-second temporal resolution is still to be unlocked and should be a main goal for the near future.

Declarations

Competing interests The authors declare no competing interests.

References

Hell SW et al (2007) Far-field optical nanoscopy. Science 316:1153–1158. https://doi.org/10.1126/science.1137395

Hell SW (2015) Nanoscopy with Focused Light (Nobel Lecture). Angew Chemie Int Ed 54:8054–8066. https://doi.org/10.1002/anie.201504181

Klar TA, Jakobs S, Dyba M, Egner A, Hell SW (2000) Fluorescence microscopy with diffraction resolution barrier broken by stimulated emission. Proc Natl Acad Sci 97:8206–8210. https://doi.org/10.1073/pnas.97.15.8206

Hell SW, Wichmann J (1994) Breaking the diffraction resolution limit by stimulated emission: stimulated-emission-depletion fluorescence microscopy. Opt Lett 19:780–782. https://doi.org/10.1364/OL.19.000780

Hofmann M, Eggeling C, Jakobs S, Hell SW (2005) Breaking the diffraction barrier in fluorescence microscopy at low light intensities by using reversibly photoswitchable proteins. Proc Natl Acad Sci 102:17565–17569. https://doi.org/10.1073/pnas.0506010102

Hell SW, Jakobs S, Kastrup L (2003) Imaging and writing at the nanoscale with focused visible light through saturable optical transitions. Appl Phys A Mater Sci Process 77:859–860. https://doi.org/10.1007/s00339-003-2292-4

Rust MJ, Bates M, Zhuang X (2006) Sub-diffraction-limit imaging by stochastic optical reconstruction microscopy (STORM). Nat Methods 3:793–796. https://doi.org/10.1038/nmeth929

Betzig E et al (2006) Imaging intracellular fluorescent proteins at nanometer resolution. Science 313:1642–1645. https://doi.org/10.1126/science.1127344

Huang B, Bates M, Zhuang X (2009) Super-resolution fluorescence microscopy. Annu Rev Biochem 78:993–1016. https://doi.org/10.1146/annurev.biochem.77.061906.092014

Sahl SJ, Hell SW, Jakobs S (2017) Fluorescence nanoscopy in cell biology. Nat Rev Mol Cell Biol 18:685–701. https://doi.org/10.1038/nrm.2017.71

Schnitzbauer J, Strauss MT, Schlichthaerle T, Schueder F, Jungmann R (2017) Super-resolution microscopy with DNA-PAINT. Nat Protoc 12:1198–1228. https://doi.org/10.1038/nprot.2017.024

Jungmann R et al (2010) Single-molecule kinetics and super-resolution microscopy by fluorescence imaging of transient binding on DNA origami. Nano Lett 10:4756–4761. https://doi.org/10.1021/nl103427w

Dai M, Jungmann R, Yin P (2016) Optical imaging of individual biomolecules in densely packed clusters. Nat Nanotechnol 11:798–807. https://doi.org/10.1038/nnano.2016.95

Strauss S et al (2018) Modified aptamers enable quantitative sub-10-nm cellular DNA-PAINT imaging. Nat Methods 15:685–688. https://doi.org/10.1038/s41592-018-0105-0

Strauss S, Jungmann R (2020) Up to 100-fold speed-up and multiplexing in optimized DNA-PAINT. Nat Methods 17:789–791. https://doi.org/10.1038/s41592-020-0869-x

Balzarotti F et al (2017) Nanometer resolution imaging and tracking with minimal photon fluxes. Science 355:606–612. https://doi.org/10.1126/science.aak9913

Masullo LA et al (2021) Pulsed Interleaved MINFLUX. Nano Lett 21:840–846. https://doi.org/10.1021/acs.nanolett.0c04600

Jouchet P et al (2021) Nanometric axial localization of single fluorescent molecules with modulated excitation. Nat Photonics 15:297–304. https://doi.org/10.1038/s41566-020-00749-9

Gu L et al (2019) Molecular resolution imaging by repetitive optical selective exposure. Nat Methods 16:1114–1118. https://doi.org/10.1038/s41592-019-0544-2

Cnossen J et al (2020) Localization microscopy at doubled precision with patterned illumination. Nat Methods 17:59–63. https://doi.org/10.1038/s41592-019-0657-7

Reymond L et al (2019) SIMPLE: Structured illumination based point localization estimator with enhanced precision. Opt Express 27:24578. https://doi.org/10.1364/OE.27.024578

Reymond L, Huser T, Ruprecht V, Wieser S (2020) Modulation-enhanced localization microscopy. J Phys Photonics 2:041001. https://doi.org/10.1088/2515-7647/ab9eac

Masullo LA, Lopez LF, Stefani FD (2021) A common framework for single-molecule localization using sequential structured illumination. Biophysical Reports, accepted. https://doi.org/10.1016/j.bpr.2021.100036

Huang F et al (2016) Ultra-high resolution 3D imaging of whole cells. Cell 166:1028–1040. https://doi.org/10.1016/j.cell.2016.06.016

Shtengel G et al (2009) Interferometric fluorescent super-resolution microscopy resolves 3D cellular ultrastructure. Proc Natl Acad Sci 106:3125–3130. https://doi.org/10.1073/pnas.0813131106

Aquino D et al (2011) Two-color nanoscopy of three-dimensional volumes by 4Pi detection of stochastically switched fluorophores. Nat Methods 8:353–359. https://doi.org/10.1038/nmeth.1583

Szalai AM et al (2021) Three-dimensional total-internal reflection fluorescence nanoscopy with nanometric axial resolution by photometric localization of single molecules. Nat Commun 12:517. https://doi.org/10.1038/s41467-020-20863-0

Bourg N et al (2015) Direct optical nanoscopy with axially localized detection. Nat Photonics 9:587–593. https://doi.org/10.1038/nphoton.2015.132

Dasgupta A et al (2021) Direct supercritical angle localization microscopy for nanometer 3D superresolution. Nat Commun 12:1180. https://doi.org/10.1038/s41467-021-21333-

Chizhik AI, Rother J, Gregor I, Janshoff A, Enderlein J (2014) Metal-induced energy transfer for live cell nanoscopy. Nat Photonics 8:124–127. https://doi.org/10.1038/nphoton.2013.345

Ghosh A et al (2019) Graphene-based metal-induced energy transfer for sub-nanometre optical localization. Nat Photonics 13:860–865. https://doi.org/10.1038/s41566-019-0510-7

Kaminska I et al (2019) Distance dependence of single-molecule energy transfer to graphene measured with DNA origami nanopositioners. Nano Lett 19:4257–4262. https://doi.org/10.1021/acs.nanolett.9b00172

Kamińska I et al (2021) Graphene energy transfer for single-molecule biophysics, biosensing, and super-resolution microscopy. Adv Mater 33:2101099. https://doi.org/10.1002/adma.202101099

Gwosch KC et al (2020) MINFLUX nanoscopy delivers 3D multicolor nanometer resolution in cells. Nat Methods 17:217–224. https://doi.org/10.1038/s41592-019-0688-

Gu L et al (2021) Molecular-scale axial localization by repetitive optical selective exposure. Nat Methods 18:369–373. https://doi.org/10.1038/s41592-021-01099-2

Huang B, Wang W, Bates M, Zhuang X (2008) Three-dimensional super-resolution imaging by stochastic optical reconstruction microscopy. Science 319:810–813. https://doi.org/10.1126/science.1153529

Willig KI, Harke B, Medda R, Hell SW (2007) STED microscopy with continuous wave beams. Nat Methods 4:915–918. https://doi.org/10.1038/nmeth1108

Rittweger E, Han KY, Irvine SSE, Eggeling C, Hell SW (2009) STED microscopy reveals crystal colour centres with nanometric resolution. Nat Photonics 3:1–4. https://doi.org/10.1038/nphoton.2009.2

Heilemann M et al (2008) Subdiffraction-resolution fluorescence imaging with conventional fluorescent probes. Angew Chemie Int Ed 47:6172–6176. https://doi.org/10.1002/anie.200802376

Nieuwenhuizen RPJJ et al (2013) Measuring image resolution in optical nanoscopy. Nat Methods 10:557–562. https://doi.org/10.1038/nmeth.2448

Descloux A, Grußmayer KS, Radenovic A (2019) Parameter-free image resolution estimation based on decorrelation analysis. Nat Methods 16:918–924. https://doi.org/10.1038/s41592-019-0515-7

Descloux AC, Grußmayer KS, Radenovic A (2021) Parameter-free rendering of single-molecule localization microscopy data for parameter-free resolution estimation. Commun Biol 4:550. https://doi.org/10.1038/s42003-021-02086-1

Schmied JJ et al (2014) DNA origami–based standards for quantitative fluorescence microscopy. Nat Protoc 9:1367–1391. https://doi.org/10.1038/nprot.2014.079

Scheckenbach M, Bauer J, Zähringer J, Selbach F, Tinnefeld P (2020) DNA origami nanorulers and emerging reference structures. APL Mater 8:110902. https://doi.org/10.1063/5.0022885

Schlichthaerle T et al (2019) Direct visualization of single nuclear pore complex proteins using genetically-encoded probes for DNA-PAINT. Angew Chemie Int Ed 58:13004–13008. https://doi.org/10.1002/anie.201905685

Thevathasan JV et al (2019) Nuclear pores as versatile reference standards for quantitative superresolution microscopy. Nat Methods 16:1045–1053. https://doi.org/10.1038/s41592-019-0574-9

von Appen A et al (2015) In situ structural analysis of the human nuclear pore complex. Nature 526:140–143. https://doi.org/10.1038/nature15381

Loïodice I et al (2004) The entire Nup107-160 complex, including three new members, is targeted as one entity to kinetochores in mitosis. Mol Biol Cell 15:3333–3344. https://doi.org/10.1091/mbc.e03-12-0878

Heydarian H et al (2021) 3D particle averaging and detection of macromolecular symmetry in localization microscopy. Nat Commun 12:2847. https://doi.org/10.1038/s41467-021-22006-5

Schmidt R et al (2021) MINFLUX nanometer-scale 3D imaging and microsecond-range tracking on a common fluorescence microscope. Nat Commun 12:1478. https://doi.org/10.1038/s41467-021-21652-z

Li Y et al (2018) Real-time 3D single-molecule localization using experimental point spread functions. Nat Methods 15:367–369. https://doi.org/10.1038/nmeth.4661

Wang Y et al (2014) Localization events-based sample drift correction for localization microscopy with redundant cross-correlation algorithm. Opt Express 22:15982–15991. https://doi.org/10.1364/OE.22.015982

Balinovic A, Albrecht D, Endesfelder U (2019) Spectrally red-shifted fluorescent fiducial markers for optimal drift correction in localization microscopy. J Phys D Appl Phys 52:204002. https://doi.org/10.1088/1361-6463/ab0862

Carter AR et al (2007) Stabilization of an optical microscope to 0.1 nm in three dimensions. Appl Opt 46:421–427. https://doi.org/10.1364/AO.46.000421

Pertsinidis A, Zhang Y, Chu S (2010) Subnanometre single-molecule localization, registration and distance measurements. Nature 466:647–651. https://doi.org/10.1038/nature09163

Coelho S et al (2020) Ultraprecise single-molecule localization microscopy enables in situ distance measurements in intact cells. Sci Adv 6:eaay8271. https://doi.org/10.1126/sciadv.aay8271

Ganji M, Schlichthaerle T, Eklund AS, Strauss S, Jungmann R (2021) Quantitative assessment of labeling probes for super-resolution microscopy using designer DNA nanostructures. ChemPhysChem 22:911–914. https://doi.org/10.1002/cphc.202100185

Früh SM et al (2021) Site-specifically-labeled antibodies for super-resolution microscopy reveal in situ linkage errors. ACS Nano 15:12161–12170. https://doi.org/10.1021/acsnano.1c03677

Ries J, Kaplan C, Platonova E, Eghlidi H, Ewers H (2012) A simple, versatile method for GFP-based super-resolution microscopy via nanobodies. Nat Methods 9:582–584. https://doi.org/10.1038/nmeth.1991

Pleiner T et al (2015) Nanobodies: site-specific labeling for super-resolution imaging, rapid epitope-mapping and native protein complex isolation. Elife 4:e11349. https://doi.org/10.7554/eLife.11349

Schlichthaerle T et al (2018) Site-Specific Labeling of Affimers for DNA-PAINT Microscopy. Angew Chemie Int Ed 57:11060–11063. https://doi.org/10.1002/anie.201804020

Wang L, Frei MS, Salim A, Johnsson K (2019) Small-molecule fluorescent probes for live-cell super-resolution microscopy. J Am Chem Soc 141:2770–2781. https://doi.org/10.1021/jacs.8b11134

Keppler A et al (2003) A general method for the covalent labeling of fusion proteins with small molecules in vivo. Nat Biotechnol 21:86–89. https://doi.org/10.1038/nbt765

Los GV et al (2008) HaloTag: a novel protein labeling technology for cell imaging and protein analysis. ACS Chem Biol 3:373–382. https://doi.org/10.1021/cb800025k

Tiede C et al (2017) Affimer proteins are versatile and renewable affinity reagents. Elife 6:e24903. https://doi.org/10.7554/eLife.24903

Opazo F et al (2012) Aptamers as potential tools for super-resolution microscopy. Nat Methods 9:938–939. https://doi.org/10.1038/nmeth.2179

Bedford R et al (2017) Alternative reagents to antibodies in imaging applications. Biophys Rev 9:299–308. https://doi.org/10.1007/s12551-017-0278-2

Lukinavičius G et al (2014) Fluorogenic probes for live-cell imaging of the cytoskeleton. Nat Methods 11:731–733. https://doi.org/10.1038/nmeth.2972

Lukinavičius G et al (2013) A near-infrared fluorophore for live-cell super-resolution microscopy of cellular proteins. Nat Chem 5:132–139. https://doi.org/10.1038/nchem.1546

D'Este E et al (2015) STED nanoscopy reveals the ubiquity of sub-cortical cytoskeleton periodicity in living neurons. Cell Rep 10:1246–1251. https://doi.org/10.1016/j.celrep.2015.02.007

Dancker P, Löw I, Hasselbach W, Wieland T (1975) Interaction of actin with phalloidin: polymerization and stabilization of F-actin. Biochim Biophys Acta 400:407–414. https://doi.org/10.1016/0005-2795(75)90196-8

Hern J, a, et al (2010) Formation and dissociation of M1 muscarinic receptor dimers seen by total internal reflection fluorescence imaging of single molecules. Proc Natl Acad Sci U S A 107:2693–2698. https://doi.org/10.1073/pnas.0907915107

Cai M et al (2004) Real time differentiation of G-Protein Coupled Receptor (GPCR) agonist and antagonist by two photon fluorescence laser microscopy. J Am Chem Soc 126:7160–7161. https://doi.org/10.1021/ja049473m

Szalai AM et al (2018) A fluorescence nanoscopy marker for corticotropin-releasing hormone type 1 receptor: computer design, synthesis, signaling effects, super-resolved fluorescence imaging, and: in situ affinity constant in cells. Phys Chem Chem Phys 20:29212–29220. https://doi.org/10.1039/C8CP06196C

Ha T, Tinnefeld P (2012) Photophysics of fluorescent probes for single-molecule biophysics and super-resolution imaging. Annu Rev Phys Chem 63:595–617. https://doi.org/10.1146/annurev-physchem-032210-103340

Vogelsang J et al (2010) Make them blink: probes for super-resolution microscopy. ChemPhysChem 11:2475–2490. https://doi.org/10.1002/cphc.201000189

Dempsey GTGGT, Vaughan JCJJC, Chen KHK, Bates M, Zhuang X (2011) Evaluation of fluorophores for optimal performance in localization-based super-resolution imaging. Nat Methods 8:1027–1036. https://doi.org/10.1038/nmeth.1768

van de Linde S, Heilemann M, Sauer M (2012) Live-cell super-resolution imaging with synthetic fluorophores. Annu Rev Phys Chem 63:519–540. https://doi.org/10.1146/annurev-physchem-032811-112012

Vogelsang J et al (2008) A reducing and oxidizing system minimizes photobleaching and blinking of fluorescent dyes. Angew Chemie 47:5465–5469. https://doi.org/10.1002/anie.200801518

Cordes T, Vogelsang J, Tinnefeld P (2009) On the mechanism of Trolox as antiblinking and antibleaching reagent. J Am Chem Soc 131:5018–5019. https://doi.org/10.1021/ja809117z

Harada Y, Sakurada K, Aoki T, Thomas DD, Yanagida T (1990) Mechanochemical coupling in actomyosin energy transduction studied by in vitro movement assay. J Mol Biol 216:49–68. https://doi.org/10.1016/S0022-2836(05)80060-9

Aitken CE, Marshall RA, Puglisi JD (2008) An oxygen scavenging system for improvement of dye stability in single-molecule fluorescence experiments. Biophys J 94:1826–1835. https://doi.org/10.1529/biophysj.107.117689

Szalai AM et al (2021) Super-resolution imaging of energy transfer by intensity-based STED-FRET. Nano Lett 21:2296–2303. https://doi.org/10.1021/acs.nanolett.1c00158

Kasper R et al (2010) Single-molecule STED microscopy with photostable organic fluorophores. Small 6:1379–1384. https://doi.org/10.1002/smll.201000203

Blumhardt P et al (2018) Photo-induced depletion of binding sites in DNA-PAINT microscopy. Molecules 23:3165. https://doi.org/10.3390/molecules23123165

Olivier N, Keller D, Gönczy P, Manley S (2013) Resolution doubling in 3D-STORM imaging through improved buffers. PLoS ONE 8:e69004. https://doi.org/10.1371/journal.pone.0069004

Schueder F et al (2019) An order of magnitude faster DNA-PAINT imaging by optimized sequence design and buffer conditions. Nat Methods 16:1101–1104. https://doi.org/10.1038/s41592-019-0584-7

Civitci F et al (2020) Fast and multiplexed superresolution imaging with DNA-PAINT-ERS. Nat Commun 11:4339. https://doi.org/10.1038/s41467-020-18181-6

Chung KKH et al (2020) Fluorogenic probe for fast 3D whole-cell DNA-PAINT. bioRxiv 2020.04.29.066886. https://doi.org/10.1101/2020.04.29.066886

Lee J, Park S, Kang W, Hohng S (2017) Accelerated super-resolution imaging with FRET-PAINT. Mol Brain 10:63. https://doi.org/10.1186/s13041-017-0344-5

Auer A, Strauss MT, Schlichthaerle T, Jungmann R (2017) Fast, background-free DNA-PAINT imaging using FRET-based probes. Nano Lett 17:6428–6434. https://doi.org/10.1021/acs.nanolett.7b03425

Mortensen KI, Churchman LS, Spudich JA, Flyvbjerg H (2010) Optimized localization analysis for single-molecule tracking and super-resolution microscopy. Nat Methods 7:377–381. https://doi.org/10.1038/nmeth.1447

Huang F et al (2013) Video-rate nanoscopy using sCMOS camera–specific single-molecule localization algorithms. Nat Methods 10:653–658. https://doi.org/10.1038/nmeth.2488

Westphal V et al (2008) Video-rate far-field optical nanoscopy dissects synaptic vesicle movement. Science 320:246–249. https://doi.org/10.1126/science.1154228

Bergermann F, Alber L, Sahl SJ, Engelhardt J, Hell SW (2015) 2000-fold parallelized dual-color STED fluorescence nanoscopy. Opt Express 23:211. https://doi.org/10.1364/OE.23.000211

Masullo LA et al (2018) Enhanced photon collection enables four dimensional fluorescence nanoscopy of living systems. Nat Commun 9:3281. https://doi.org/10.1038/s41467-018-05799-w

Bodén A et al (2021) Volumetric live cell imaging with three-dimensional parallelized RESOLFT microscopy. Nat Biotechnol 39:609–618. https://doi.org/10.1038/s41587-020-00779-2

Ouyang W, Aristov A, Lelek M, Hao X, Zimmer C (2018) Deep learning massively accelerates super-resolution localization microscopy. Nat Biotechnol 36:460–468. https://doi.org/10.1038/nbt.4106

Filius M et al (2020) High-speed super-resolution imaging using protein-assisted DNA-PAINT. Nano Lett 20:2264–2270. https://doi.org/10.1021/acs.nanolett.9b04277

Enderlein J (2000) Tracking of fluorescent molecules diffusing within membranes. Appl Phys B Lasers Opt 71:773–777. https://doi.org/10.1007/s003400000409

Weigel AV, Simon B, Tamkun MM, Krapf D (2011) Ergodic and nonergodic processes coexist in the plasma membrane as observed by single-molecule tracking. Proc Natl Acad Sci 108:6438–6443. https://doi.org/10.1073/pnas.1016325108

Sako Y, Minoghchi S, Yanagida T (2000) Single-molecule imaging of EGFR signalling on the surface of living cells. Nat Cell Biol 2:168–172. https://doi.org/10.1038/35004044

Eilers Y, Ta H, Gwosch KC, Balzarotti F, Hell SW (2018) MINFLUX monitors rapid molecular jumps with superior spatiotemporal resolution. Proc Natl Acad Sci 115:6117–6122. https://doi.org/10.1073/pnas.1801672115

Piston DW, Kremers G-J (2007) Fluorescent protein FRET: the good, the bad and the ugly. Trends Biochem Sci 32:407–414. https://doi.org/10.1016/j.tibs.2007.08.003

Lerner E et al (2018) Toward dynamic structural biology: two decades of single-molecule Förster resonance energy transfer. Science 359:eaan1133. https://doi.org/10.1126/science.aan1133

Deußner-Helfmann NS et al (2018) Correlative single-molecule FRET and DNA-PAINT imaging. Nano Lett 18:4626–4630. https://doi.org/10.1021/acs.nanolett.8b02185

Fernández-Suárez M, Ting AY (2008) Fluorescent probes for super-resolution imaging in living cells. Nat Rev Mol Cell Biol 9:929–943. https://doi.org/10.1038/nrm2531

Grimm JB et al (2020) A general method to optimize and functionalize red-shifted rhodamine dyes. Nat Methods 17:815–821. https://doi.org/10.1038/s41592-020-0909-6

Chen F, Tillberg PW, Boyden ES (2015) Expansion microscopy. Science 347:543–548. https://doi.org/10.1126/science.1260088

Mau A, Friedl K, Leterrier C, Bourg N, Lévêque-Fort S (2021) Fast widefield scan provides tunable and uniform illumination optimizing super-resolution microscopy on large fields. Nat Commun 12:3077. https://doi.org/10.1038/s41467-021-23405-4

Stehr F, Stein J, Schueder F, Schwille P, Jungmann R (2019) Flat-top TIRF illumination boosts DNA-PAINT imaging and quantification. Nat Commun 10:1268. https://doi.org/10.1038/s41467-019-09064-6

Pape JK et al (2020) Multicolor 3D MINFLUX nanoscopy of mitochondrial MICOS proteins. Proc Natl Acad Sci 117:20607–20614. https://doi.org/10.1073/pnas.2009364117

Tardif C et al (2019) Fluorescence lifetime imaging nanoscopy for measuring Förster resonance energy transfer in celular nanodomains. Neurophotonics 6: 015002. https://doi.org/10.1117/1.NPh.6.1.015002